A Numerical Method For Fluidelastic Instability Evaluation In Nuclear Reactor System And Plant Components

D. P. Weber[(1)], R. Brewster[(2)], S. S. Chen[(1)] and T. Y. C. Wei[(1)]

[(1)] Argonne National Laboratory, Argonne, IL
[(2)] adapco, Inc., Melville, NY

ABSTRACT

Fluidelastic instability of reactor system and plant components is very important and full of rich dynamic interaction phenomena. It has been studied extensively during the past quarter of the century. Various mathematical models have been developed to predict the instability flow velocity. The key elements necessary to predict fluidelastic instability accurately are motion-dependent fluid-force coefficients, which are traditionally obtained analytically or experimentally. This paper presents a computational fluid dynamics (CFD) method to calculate motion-dependent fluid-force coefficients including added mass, fluid damping and fluid stiffness, based on the unsteady-flow theory. Using the mathematical model and the characteristics of motion-dependent fluid-force coefficients, we can predict component response more cost efficiently and provides additional insights into fluidelastic instability under various conditions.

INTRODUCTION

Reactor system and plant components submerged in flow or conveying fluid can be subjected to dynamic instability, typically referred to as fluidelastic instability. The threshold flow velocity at which a component begins to undergo large oscillations is called the critical flow velocity. If a component is operated at a flow velocity above the critical value, severe damage to the components is likely to occur, often after only a short time of operation. Therefore, it is not acceptable to operate a component at a flow velocity greater than the critical value [1, 2].

Since the advent of commercial nuclear energy, nuclear power engineers have been faced with flow-induced vibration and instability problems in nuclear system components [3, 4, 5, 6, 7]. Although the problems are not overwhelming and generally not considered as a major aspect of the design, there is no doubt that flow-induced vibration and instability problems in nuclear power stations will continue to receive considerable attention because of economic loss, safety, and past costly incidents [8, 9, 10, 11].

This fascinating and complex topic continues to be in the forefront of structural and fluid mechanics, encompassing fluid dynamics, structural engineering, vibration, and nonlinear science. Experts in this field have provided vital research that has had a pivotal effect on the useful life of equipment in various industries. At present, not all of the physics associated with fluidelastic instability are well understood. There remains a series of unsettled issues. The present state of knowledge in this area is far from complete. This paper will present a method to model the dynamic characteristics of the coupled media using unsteady flow theory and the CFD code, STAR-CD, in the prediction of system response. The goal is to provide the key elements required for application of the unsteady flow theory and to develop a design tool for industry to use in addressing important issues.

Mathematical Models for Fluidelastic Instability

There are several approaches to these types of fluidelastic instability problems: (1) Empirical Correlations - prediction of response of structures in flow is based on empirical correlations established experimentally. The detailed excitation mechanism and the physics of dynamic fluid/structure interactions are not studied [12, 13]. (2) Complete Coupled Fluid-Structure Model - Using the theory of elasticity, linear or nonlinear, and the Navier-Stokes equations to predict the response of the coupled system directly. Using this method, the fluid forces are not quantified explicitly as they depend on structural motions [14, 15]. (3) Simplified Coupled Fluid-Structure Model - The fluid forces are quantified in terms of incoming flow field and structural motion. The techniques in quantifying motion-dependent fluid forces and flow excitation forces can be analytical methods, experimental techniques or CFD [16, 17, 18].

All these methods have been used in various industries and each method has its advantages and disadvantages. For complicated components such as fuel bundles composed of many fuel rods, the problems do not lend themselves to first principles modeling and the design is heavily reliant on empirical correlations or past experience [12]. For simple components, such as a thermocouple or a chimney in crossflow, the complete coupled fluid-structure model can be used [19]. The simplified coupled model possesses the advantages of the two previous models if it is applied intelligently in the design of complicated structures. This is the method used in this study.

Mathematically, different types of fluid/structure response can be described by a standard equation [2]:

$$[M_s + M_f]\{\ddot{Q}\} + [C_s + C_f]\{\dot{Q}\} + [K_s + K_f]\{Q\} = \{G\} \quad (1)$$

where $\{Q\}$, $\{\dot{Q}\}$, and $\{\ddot{Q}\}$ are generalized structural displacement, velocity, and acceleration, respectively; mass matrices include structural mass $[M_s]$ and added mass $[M_f]$; damping matrices include structural damping $[C_s]$ and fluid damping $[C_f]$; stiffness matrices include structural stiffness $[K_s]$ and fluid stiffness $[K_f]$; and $\{G\}$ is the other excitation forces [20]. Different types of instability can be classified according to the dominant terms in Eq. 1. (1) Fluid-damping-controlled instability (single mode flutter): The dominant terms are associated with the symmetric portion of damping matrix C_f. Flutter arises because the fluid damping forces create negative damping. (2) Fluid-stiffness-controlled instability (coupled-mode flutter): The dominant terms are associated with the antisymmetric portion of the stiffness matrix K_f.

Fluid added-mass and the damping and stiffness matrices, are functions of motion-dependent fluid-force coefficients. Quantification of these coefficients based on different approximations has been attempted. These approximations are limited to specific geometries and are valid in specific parameter ranges. At this time, there is an urgent need to develop comprehensive data that can be applied to general cases. Without data that are applicable to general cases, component failures have occurred, some with safety hazard potential and all with significant economic loss. For example, the motion-dependent fluid forces acting on tube bundles have led to catastrophic failures in heat exchangers and high maintenance and repair costs for steam generators.

Motion-Dependent Fluid-Force Coefficients Based on CFD

To complete the simplified coupled fluid-structure model, it is important to incorporate the fluid forces accurately. Motion-dependent fluid forces depend on deviation from a reference state of steady flow, and can be grouped according to three theories [20]:quasistatic-flow theory - motion-dependent fluid forces attributed to structure position only [21, 22]; quasisteady-flow theory - fluid forces attributed to variations in structure velocity in addition to its position [23, 24]; unsteady-flow theory - the unsteady fluid forces acting on the structure being the same as those acting on the structure that is undergoing periodic oscillations [17, 25] At this point in time, CFD has rarely been used to obtain the key elements of motion-dependent fluid forces particularly for practical applications. Using CFD is expected to be the most fruitful way for nuclear reactor designs. This study presents a CFD method that is based on the unsteady-flow theory.

To demonstrate the technique, consider a group of n tubes vibrating in a flow, as shown in Fig. 1. The axes of the tubes are parallel to one another and perpendicular to the x-y plane. The radius R of each tube is the same, and the fluid is flowing with a gap flow velocity U. The displacement components of Tube j in the x and y directions are u_j and v_j, respectively. The motion-dependent fluid-force components acting on Tube j in the x and y directions are, respectively, g_j and h_j, and are given [2, 20] as

$$g_j = -\rho\pi R^2 \sum_{k=1}^{n}\left(\alpha_{jk}\frac{\partial^2 u_k}{\partial t^2} + \sigma_{jk}\frac{\partial^2 v_k}{\partial t^2}\right) + \frac{\rho U^2}{\omega}\sum_{k=1}^{n}\left(\alpha'_{jk}\frac{\partial u_k}{\partial t} + \sigma'_{jk}\frac{\partial v_k}{\partial t}\right)$$

$$+ \rho U^2 \sum_{k=1}^{n}\left(\alpha''_{jk}u_k + \sigma''_{jk}v_k\right) \quad (2)$$

and

$$h_j = -\rho\pi R^2 \sum_{k=1}^{n}\left(\tau_{jk}\frac{\partial^2 u_k}{\partial t^2} + \beta_{jk}\frac{\partial^2 v_k}{\partial t^2}\right) + \frac{\rho U^2}{\omega}\sum_{k=1}^{n}\left(\tau'_{jk}\frac{\partial u_k}{\partial t} + \beta'_{jk}\frac{\partial v_k}{\partial t}\right)$$

$$+ \rho U^2 \sum_{k=1}^{n}\left(\tau''_{jk}u_k + \beta''_{jk}v_k\right), \quad (3)$$

where ρ is fluid density; t is time; ω is circular frequency of tube oscillations; α_{jk}, β_{jk}, σ_{jk}, and τ_{jk} are added-mass coefficients; α'_{jk}, β'_{jk}, σ'_{jk}, and τ'_{jk} are fluid-damping coefficients; and α''_{jk}, β''_{jk}, σ''_{jk}, and τ''_{jk} are fluid-stiffness coefficients.

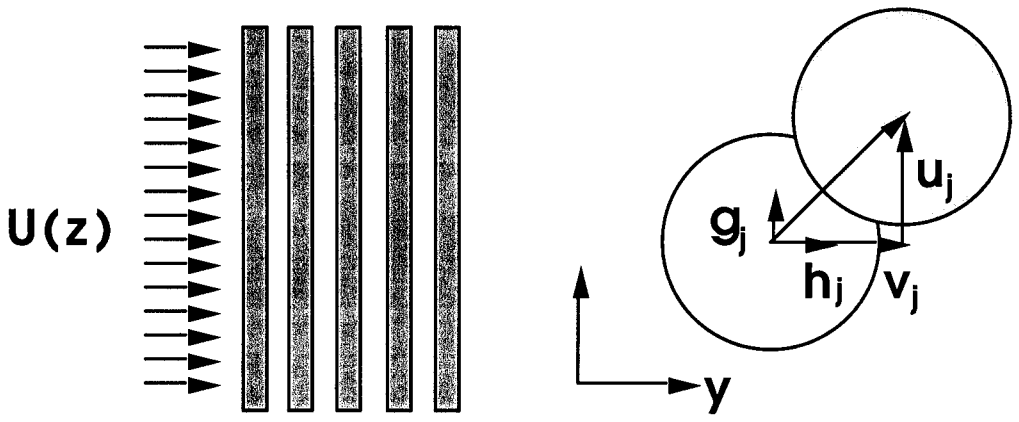

Fig. 1. Tube Array in Crossflow and Schematic Representation of Displacement Components of Tube j and Motion-Dependent Fluid-Force Components Acting on Tube j

Two methods have been used to obtain motion-dependent fluid forces: the indirect method and the direct method. The indirect method calculates fluid forces from structural responses, such as structural displacements and accelerations [26] and the direct method is to measure or calculate motion-dependent fluid forces directly [17, 25, 27]. In this study, we used the direct method, based on the unsteady-flow theory. Fluid-force coefficients can be determined by calculating the fluid forces acting on all structural elements that are due to oscillations of a particular element. For example, as shown in Fig. 1, if Tube k is excited in the x direction, its displacement in the x direction is given by

$$u_k = u \cos \omega t. \tag{4}$$

The fluid-force components acting on Tube j in the x and y directions are

$$g_j = \frac{1}{2}\rho U^2 c_{jk} \cos\left(\omega t + \phi_{jk}\right) u \tag{5}$$

and

$$h_j = \frac{1}{2}\rho U^2 d_{jk} \cos\left(\omega t + \psi_{jk}\right) u \tag{6}$$

where c_{jk} and d_{jk} are the fluid-force amplitudes and ϕ_{jk} and ψ_{jk} are the phase angles by which the fluid forces acting on Tube j lead the displacement of Tube k.
With Eqs. 2, 3, and 4, we can also write the fluid-force components as

$$g_j = \left(\rho\pi R^2 \omega^2 \alpha_{jk} + \rho U^2 \alpha''_{jk}\right) u \cos \omega t - \rho U^2 \alpha'_{jk}\, u \sin \omega t \tag{7}$$

and

$$h_j = \left(\rho\pi R^2 \omega^2 \tau_{jk} + \rho U^2 \tau''_{jk}\right) u \cos \omega t - \rho U^2 \tau'_{jk} u \sin \omega t \tag{8}$$

Combining Eqs. 5 and 7, and 6 and 8, we obtain

$$\alpha''_{jk} = \frac{1}{2} c_{jk} \cos\phi_{jk} - \frac{\pi^3}{Ur^2} \alpha_{jk}$$

$$\tau''_{jk} = \frac{1}{2} d_{jk} \cos\psi_{jk} - \frac{\pi^3}{Ur^2} \tau_{jk}, \tag{9}$$

$$\alpha'_{jk} = \frac{1}{2} c_{jk} \sin\phi_{jk},$$

and

$$\tau'_{jk} = \frac{1}{2} d_{jk} \sin\psi_{jk}, \tag{10}$$

where Ur is the reduced flow velocity ($Ur = \pi U/\omega R$).

The added-mass coefficients α_{jk} and τ_{jk} in Eqs. 9 can be calculated by applying the potential-flow theory [2, 28] or CFD method in quiescent fluid. Then α'_{jk}, α''_{jk}, τ'_{jk}, and τ''_{jk} can be calculated from Eqs. 9 and 10 by calculating fluid force components. If Tube k is excited in the y direction, using the same technique, we can obtain force coefficients β'_{jk}, β''_{jk}, σ'_{jk}, and σ''_{jk} in the same manner.

In the past, motion-dependent fluid forces were often measured experimentally. STAR-CD is used in this study to calculate motion-dependent fluid-force coefficients. STAR-CD is a powerful CFD tool for fluids and thermal analysis and has been designed for use in a CAE environment. It contains provisions for all necessary fluid modeling aspects of complicated structural elements and is suitable for predicting a large variety of industrial fluid flow problems. It has been applied to predict vortex shedding and motion-dependent fluid forces for a single tube and fluid/structure interaction of a tube row in cross flow; the predicted Strouhal number, flow pattern, and critical flow velocity agree reasonably well with experimental data {30]. In this study, it is used to calculate the motion-dependent fluid-force coefficients for a tube row in cross flow. Using this method, these coefficients can be analyzed in a cost-effective manner.

Numerical Results from STAR-CD and Comparison with Experimental Data

The governing partial differential equations for momentum, pressure and turbulence were solved numerically in order to predict the added mass and fluid damping and stiffness coefficients. The simulations were carried out using STAR-CD, a general-purpose commercial CFD computer code suitable for predicting flows in a large variety of industrial fluid flow problems. The flows studied in this paper were assumed to be statistically two-dimensional flows, although the unsteady behavior of the flow is taken into account in the calculations.

Based upon previous experience with numerical simulations of tubes in cross-flow [30], a quadratic non-linear k-ε turbulence model, based on the turbulent (or eddy) viscosity concept, was used to model the turbulence outside of the boundary layer. Within the boundary layer, a one-equation algebraic model was used to compute the turbulence dissipation, ε. Note that the use of such a "two-layer" approach requires a dense near-wall mesh, as described below.

STAR-CD is a finite-volume based CFD code. In this study, a total of approximately 50,000 finite volumes (fluid cells) were used to model the two-dimensional flow domain. Figure 2 shows the mesh used in this study. Note the very dense near-wall mesh used to accurately capture the boundary-layer flow. Also note the use of fully unstructured meshing shown in Figure 2(b).

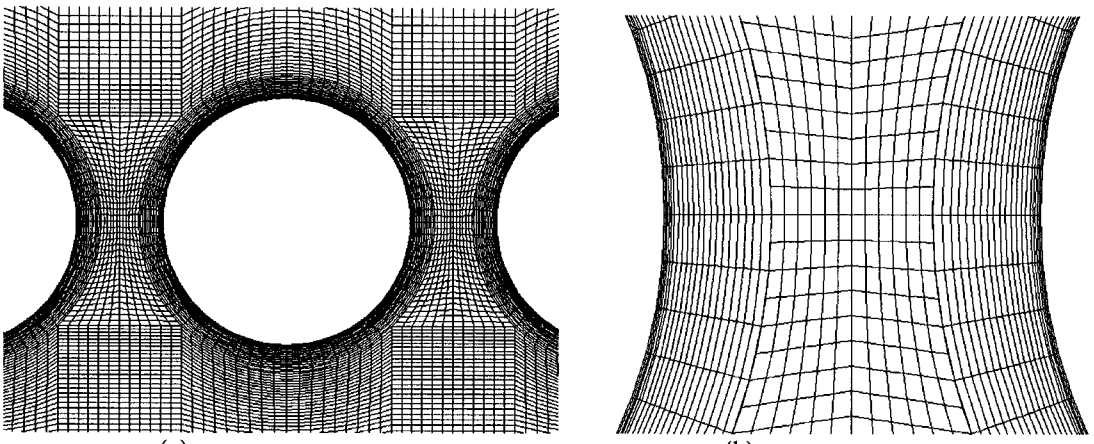

Figure 2: Computational Mesh used in CFD Calculations: (a) View of the Mesh Around One Tube; (b) Detail of Mesh Near Tube Walls

To simulate the motion of tube 1 (see Figure 3), STAR-CD's moving mesh capability was used. At each time step, the position of tube 1 can be computed from Eq. 4. STAR-CD then moves the surface nodes of tube 1 to this position. Subsequent mesh filling and smoothing operations are then used to maintain the mesh quality. Particular care was taken to preserve the quality of the near-wall mesh layers.

Spatial discretization of the convective terms in the conservation equations was accomplished using a second-order accurate bounded scheme, while the diffusive terms were discretized using a central-difference scheme, which is also second-order accurate. The equations were advanced in time using a fully implicit time stepping procedure.

Extensive measurements of motion-dependent fluid-force coefficients have been made [25, 29]. Tests have been performed for single tube, two tubes, tube rows, triangular arrays, and square arrays [17, 25, 27, 29, 31]. A tube row with the pitch-to-tube-diameter ratio (P/D) of 1.35 (tube diameter = 2.54 cm), shown in Fig. 3, is chosen for CFD calculations to compare with experimental data. The tube row is subjected to uniform water flow at room temperature. The CFD calculation procedure follows the steps given in the previous section. It includes added mass, fluid-damping and fluid stiffness coefficients.

- Fluid added-mass coefficients are calculated using the excitation frequency of 1 Hz and excitation amplitudes of 1 mm and 5 mm for tube 1 oscillating in the direction of tube row for stationary fluid.
- Fluid-damping and fluid-stiffness coefficients are calculated based on the two gap flow velocities, 0.05 m/s, and 0.19 m/s (Reynolds number equal to 1,300 and 4,950 based on the gap flow velocity), where gap velocity is Uin/(1-D/P). The tube excitation amplitude is set at 2 mm and frequencies are set at 0.05 Hz, 0.5 Hz, and 2.5 Hz for tube 1 oscillating in the lift direction.

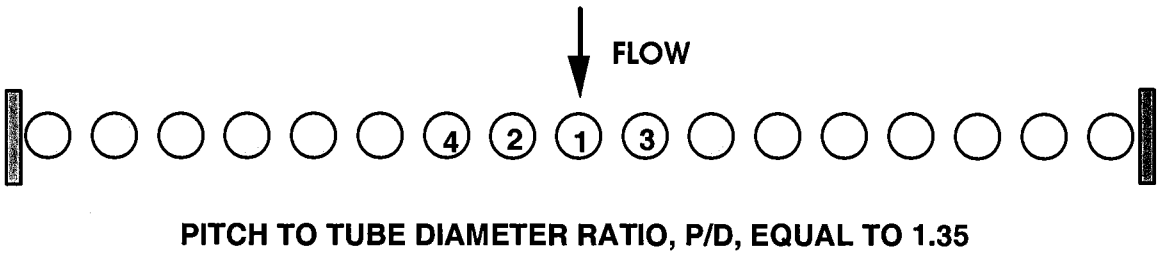

Fig. 3 A Tube Row in Crossflow

Added mass from STAR-CD, analytical solutions, and experimental data are given in Table 1. The analytical results are obtained from the potential flow theory [28]. It is noted that CFD results compare well with the experimental data and analytical solution. Due to the symmetry of the tube row, α_{21} and α_{31} are equal theoretically. CFD results agree reasonably well. Based on the theoretical results, the added mass coefficient, τ_{j1} (j=1, 2, 3, 4) equal to zero. CFD results show very

small values. The effect of oscillation amplitude from 1 mm to 5 mm is small. Table 1 shows that CFD is an efficient way to calculate added mass coefficients and the results agree well with analytical and experimental data.

Table 1. Comparison of Added Mass Coefficients (u is Excitation Amplitude)

Added Mass Coefficients	Analytical Results	CFD Results u = 1 mm	CFD Results u = 5 mm	Experimental Data u = 1 mm	Experimental Data u = 4 mm
α_{11}	1.1050	1.2225	1.2410	1.02	1.06
α_{21}	-0.2724	-0.2894	-0.3023	-0.29	-0.31
α_{31}	-0.2724	-0.2865	-0.2984	-0.28	-0.30
α_{41}	-0.0367	-0.0303	-0.0302	-0.04	-0.03
τ_{11}	0	-0.0009	-0.0009	0.04	-0.01
τ_{21}	0	0.0010	0.0001	0.04	-0.01
τ_{31}	0	-0.0025	-0.0026	0.04	0.01
τ_{41}	0	0.0026	0.0026	-0.02	-0.00

Fluid-damping and fluid-stiffness coefficients have been calculated for two flow velocities. Typical results from CFD calculations and experiments are shown in Figs. 4 and 5 for gap velocity of 0.19 m/s. Similar results were obtained for 0.05 m/s. Comparing CFD results with experimental data, it is noted:

- CFD results agree qualitatively with experimental data for both fluid-damping and fluid-stiffness coefficients. It noted that the scatter of experimental data at some reduced flow velocities is fairly large. This was partly due to the limitation of force transducers to measure motion-dependent fluid forces at low flow velocities and the unstable nature of flow field across a tube row.
- Due to the geometrical symmetry of tubes 2 and 3 with respect to flow in a tube row, the coefficients α'_{21}, α'_{31}, α''_{21}, α''_{31} are symmetrical and the coefficients τ'_{21}, τ'_{31}, τ''_{21}, τ''_{31} are asymmetrical.
- The CFD results for τ'_{21} and τ'_{31} have opposite sign from those of experimental data. A similar situation was noted in comparing different experimental data in some cases. This is believed to be associated with the jet switching phenomenon [30, 32]. When the flow pattern changes, motion-dependent fluid-force coefficients also change as the flow has bistable flow patterns.

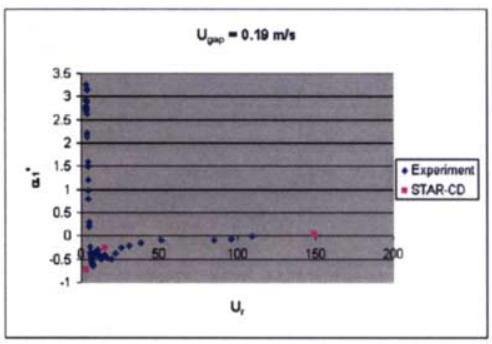

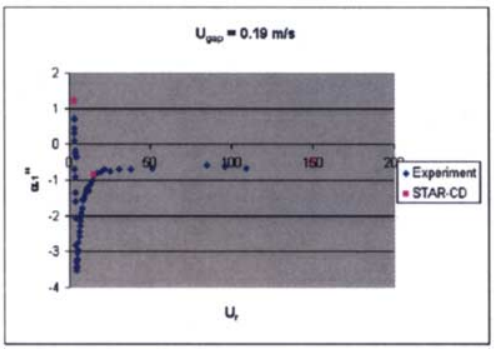

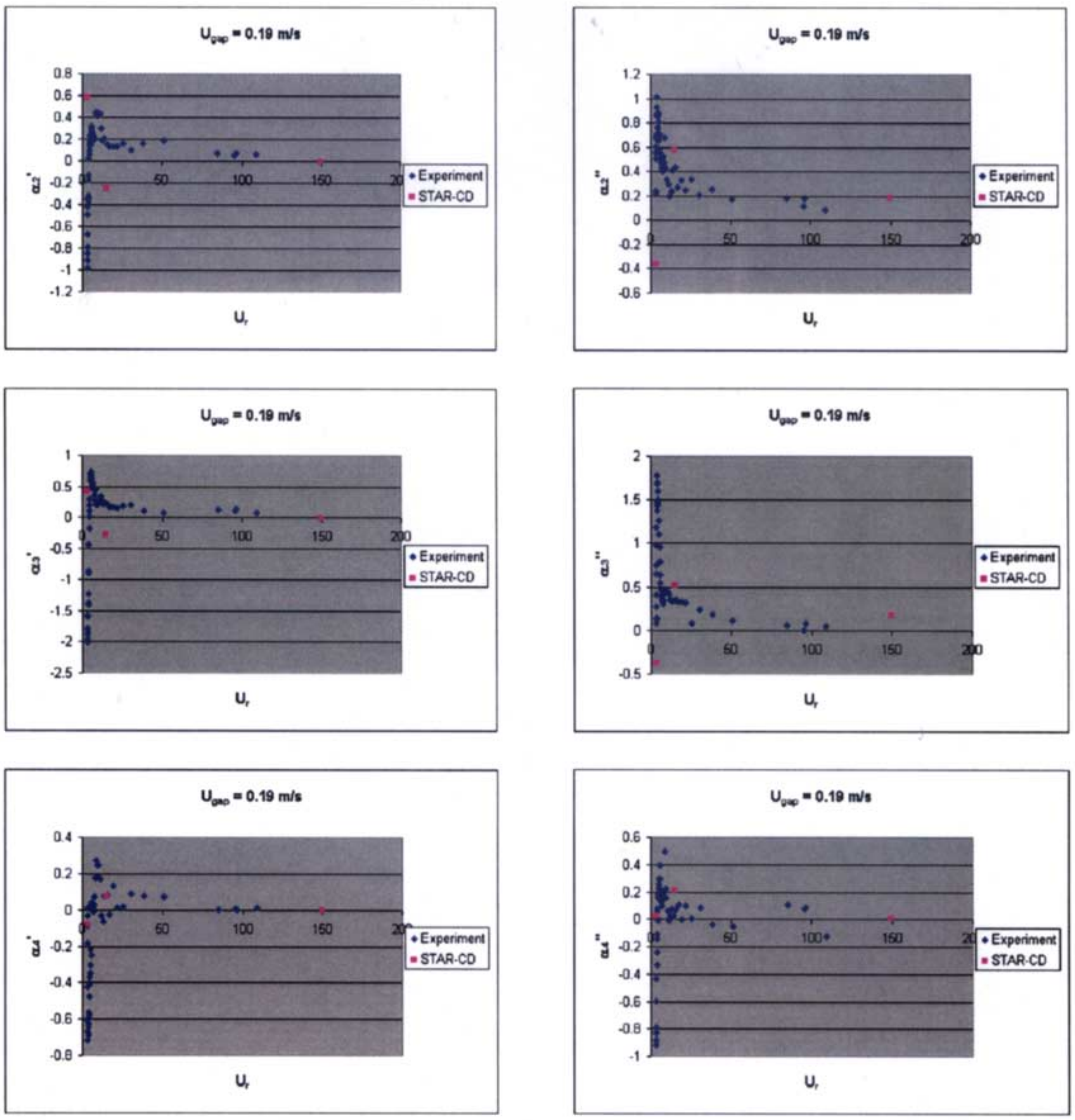

Fig. 4. Fluid-Damping and Fluid-Stiffness Coefficients α_{j1}' and α_{j1}'', j = 1, 2, 3, 4, for a Tube Row

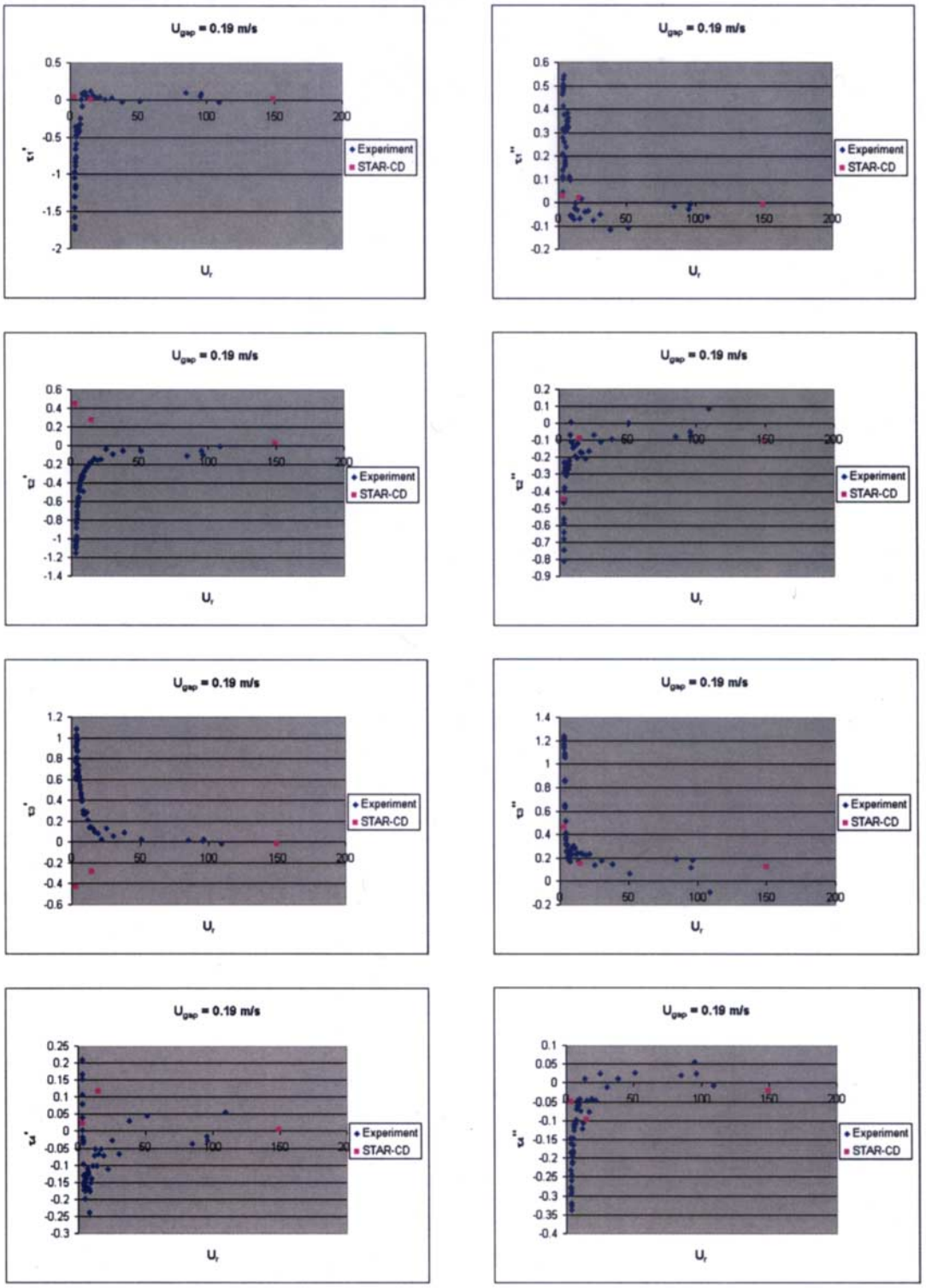

Fig. 5. Fluid-Damping and Fluid-Stiffness Coefficients τ'_{j1} and τ''_{j1}, j = 1, 2, 3, 4, for a Tube Row

The results of CFD calculations for the tube row look very promising. A tube row represents a classical case of complicated flow field and distinctive instability mechanisms [32, 33]. Additional calculations are being performed with the objective to calculate motion-dependent fluid-force coefficients accurately and efficiently. Future work will focus on the improvement and verification of the accuracy of the CFD calculations, development of coefficients for various tube arrays, effects of various system parameters, and incorporation in the mathematical model based on the unsteady flow theory for system components to predict stability, structural response, and component wear and fatigue.

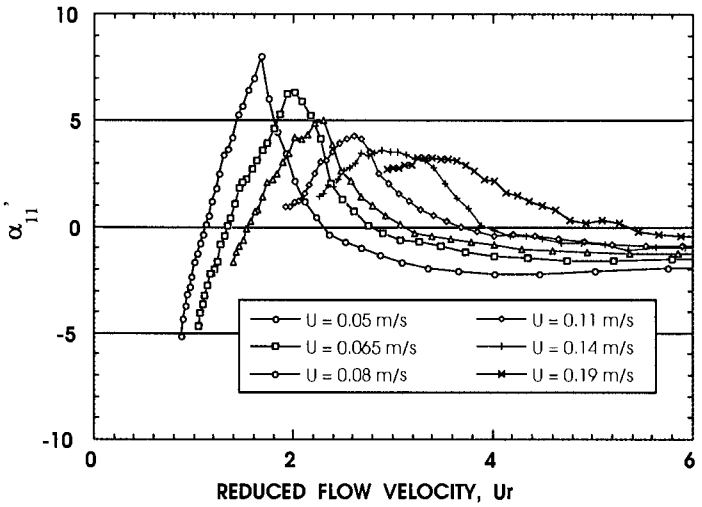

Fig. 6. Experimental Data for the Self-Induced Fluid Dumping, α_{11}', of a Tube Row as a Function of Reduced Flow Velocity for 6 Different Flow Velocities

Characteristics of Motion-Dependent Fluid-Force Coefficients and their Effects on Fluidelastic Instability

The characteristics of motion-dependent fluid-force coefficients have been evaluated from dimensional analysis of flow field and structural components, experimental data, and CFD results. Some characteristics of fluid-force coefficients are noted.

Parameters That Affect Fluid-Force Coefficients

The motion-dependent fluid-force coefficients depend on many system parameters. Based on the theoretical and experimental results, if the effects of turbulence and oscillation amplitude are ignored, any fluid-force coefficient, c, can be written as follows [20]:

$$c = c\left(\frac{P}{D}, \frac{T}{D}, Re, Ur\right). \tag{11}$$

where D = structural dimension, P/D (T/D) = longitudinal (transverse) spacing, Re = Reynolds number, and Ur = U/fD. Equation 11 is the general equation based on the unsteady-flow theory. In the quasistatic and quasisteady flow theories, the fluid-force coefficients are assumed to be independent of Re and Ur, i.e.,

$$c = c\left(\frac{P}{D}, \frac{T}{D}\right). \tag{12}$$

Earlier analytical models are based on Eq. 12. CFD results and experimental data confirm the validity of the models given in Eqs. 11 and 12 under different conditions.

Reynolds Number

In the past, Reynolds number was ignored in most cases in the prediction of motion-dependent fluid forces. Consider the tube row shown in Fig. 3. The experimental data of the self-induced damping coefficient for the six flow velocities of the tube row are shown in Fig. 6. This coefficient determines the stability of the constrained mode of the tube row [29]. The region of positive values depends on Reynolds number; its region is smaller and its peak value is larger with lower Reynolds number. Fluid-force coefficients is a function of Reynolds number. At low reduced flow velocities, Reynolds number is a parameter which can not be ignored on structural stability and response prediction.

High Ur and Quasisteady-Flow Theory

CFD results and experimental data show that at large Ur, all fluid-force coefficients are approximately constant. Thus, Eq. 12 is applicable for Ur > ~20 if the effects of oscillation amplitude, turbulence, and Reynolds number are not considered. This has a very important impact on the prediction of dynamic instability. Because fluid-force coefficients are independent of Ur, fluid-force coefficients are measured or calculated at a particular Ur only. But for small Ur, where all fluid-force coefficients depend on Ur, it is necessary to measure or calculate all fluid-force coefficients at every Ur.

Naturally, one would ask why all fluid-force coefficients are independent of Ur for Ur > ~20. We can analyze this question as follows: Consider a structure oscillating with an amplitude u sinωt. The ratio of structural velocity to flow velocity is

$$r = \frac{u\omega}{U} = \frac{2\pi\left(\frac{u}{D}\right)}{Ur}. \tag{13}$$

For small-amplitude oscillation, u/D is on the order of 0.1. If Ur > 20, r is <4%. This means the velocity of the structure is much smaller than the flow velocity. Therefore, the transient motion of the structure does not have any significant effect on the fluid-force coefficients. On the other hand, if Ur < 20, the structure velocity and flow velocity are approximately the same order of magnitude, and the fluid-force coefficients are expected to be affected significantly by the structural velocity. It is apparent that, when r is small (i.e., Ur is large), the quasisteady assumption is valid.

Symmetry and Asymmetry of Fluid Damping and Stiffness Coefficients

In many components, the structural elements used are symmetrical with respect to the incoming flow, fluid-damping and -stiffness coefficients exhibit the properties of symmetry or asymmetry. For example, for a tube row shown in Fig. 3, it is found that the coefficients α'_{21}, α'_{31}, β'_{21}, β'_{31}, α''_{21}, α''_{31} β''_{21}, β''_{31}, are symmetrical and the coefficients τ'_{21}, τ'_{31}, σ'_{21}, σ'_{31}, τ''_{21}, τ''_{31}, σ''_{21}, σ''_{31} are asymmetrical.

The initial experience has been that the symmetrical and asymmetrical properties of fluid-force coefficients for structural elements located geometrically in symmetrical positions, in most cases, follow closely what is theoretically expected. In some cases, the trend is much more unpredictable. This is believed to be due to the stability of flow patterns. This will result in differences in instability mechanisms and instability modes.

CONCLUDING REMARKS

This paper presents a numerical study of motion-dependent fluid forces that is based on the unsteady-flow theory and uses the computational fluid dynamics (CFD) code STAR-CD. A tube row with the pitch-to-tube-diameter ratio of 1.35 is analyzed and measured. From the calculated or measured fluid forces and tube motion, added-mass, fluid-damping and fluid-stiffness coefficients were obtained. The effects of oscillation amplitude, Reynolds number and reduced flow velocity are investigated. The CFD results and experimental data provide some new insights into the motion-dependent fluid forces and its effects on instability mechanisms.

At high reduced flow velocity, fluid-force coefficients are practically independent of reduced flow velocity. However, at low reduced flow velocity, fluid-damping and fluid-stiffness coefficients depend on reduced flow velocity, Reynolds number, and oscillation amplitude. Once fluid damping and stiffness coefficients are known, the response of a component can be predicted on the basis of the unsteady-flow theory. Fluid damping and fluid stiffness play an important role in determining structural response. The system may become unstable because of fluid damping, fluid stiffness, or both.

In the past, different theories have been employed in the prediction of fluidelastic instability: quasistatic-, quasisteady-, and unsteady-flow theories. Despite significant differences in the theoretical models, there is some agreement in the general conclusions obtained from the various analyses. In particular, it is shown that the most important parameter for predicting

fluidelastic instability is the unsteady nature of the flow. In these theories, some assumptions were applied; therefore, these theories are not applicable to all cases. With the unsteady-flow theory and fluid-force coefficients obtained using CFD, the analytical model of fluidelastic instability can be analyzed in detail. The tool and technique presented in this study can be applied to various cases to resolve issues of fluidelastic instability. This study demonstrates that CFD is the way to develop motion-dependent fluid-force coefficients; it is cost effective and provides the needed information which may be very difficult to obtain by other methods.

REFERENCES

1. Blevins, R. D. 1976. Flow-Induced Vibration, John Wiley & Sons, Inc., New York.
2. Chen, S. S. 1987. Flow-Induced Vibration of Circular Cylindrical Structures, Hemisphere Publishing Corp., New York.
3. Wambsganss, M. W. 1967. "Vibration of Reactor Core Components," Reactor-Fuel Process Technology, Vol. 10(1), pp. 208-219.
4. Blevins, R. D. 1979. "Flow-Induced Vibration in Nuclear Reactors: A Review." Progress in Nuclear Energy, Vol. 4, pp. 25-49.
5. Paidoussis, M. P. 1980. "Flow-Induced Vibration in Nuclear Reactors and Heat Exchangers." In Practical Experiences with Flow-Induced Vibration. Ed. E. Naudascher and D. Rockwell, pp. 1-81, Springer Verlag.
6. Axisa, F. 1993. "Flow-Induced Vibration of Nuclear System Components," in Technology for the '90s, Ed. M. K. Au-Yang, ASME Publication, pp. 897-956.
7. Pettigrew, M. J., Taylor, C. E., Fisher, N. J., and Meyer, M. J. 1996, "Flow-Induced Vibration and Fretting-Wear Damage in a Moisture Separator Reheater," ASME Publication, PVP-Vol. 328, pp. 59 - 74.
8. Reisch, F. 1982. "Technical Note: New Type of Steam Generator Fails in First Year of Operation." Nuclear Safety, Vol. 23(3), pp. 355-358.
9. Yamaguchi, A., Morishita, M., Wada, Y., Iwata, K., and Ichimiya, M. 1997. "Failure Mechanism of a Thermocouple Well Caused by Flow-Induced Vibration." ASME, 4th Int. Sym. on Fluid-Structure Interactions, Aeroelasticity, Flow-Induced Vibration and Noise, Vol. 1. pp. 139-148.
10. Guerout, F. M., and Fisher, N. J. 1999. "Steam Generator Fretting-Wear Damage: A Summary of Recent Findings," in Flow-Induced Vibration-1999, ASME Publication, PVP-Vol. 389, pp. 227-234.
11. Peters, M. and Bokhorst, E. 2000, "Flow-Induced Pulsations in Pipe Systems with Closed Branches, Impact of Flow Direction," in Flow Induced Vibration, Ed. by S. Ziada and T. Staubli, A. A. Balkema/Rotterdam/Brookfield, pp. 669-676.
12. Paidoussis, M. P. 1965. "The Amplitude of Fluid-Induced Vibration of Cylinders in Axial Flow," AECL-2225, Atomic Energy of Canada Limited, Chalk River, Ontario, Canada.
13. Chen, Y. N. and Weber, M. 1972. "Flow-Induced Vibrations in Tube Bundle Heat Exchangers with Cross and Parallel Flow," ASME Symposium on Flow-Induced Vibration in Heat Exchangers, New York, December 1970, pp. 57-77.
14. Kassera, V., and Strohmeier, K. 1996. "Simulation of Cross Flow Induced Tube Bundle Vibrations," ASME Publication, PVP-Vol. 328, pp. 39-52.
15. Bendiksen, O. 1997. "Fluid-Structure Coupling Requirements for Time-Accurate Aeroelastic Simulations," ASME Publication AD-Vol. 53-3, pp. 89-104.
16. Chen, S. S., and Wambsganss, M. W. 1972. "Parallel-Flow-Induced Vibration of Fuel Rods," Nuclear Engineering and Design, Vol. 18, pp. 253-278.
17. Tanaka, H., Takahara, S., and Ohta, K. 1982. "Flow-Induced Vibration of Tube Arrays with Various Pitch-to-Diameter Ratios," Trans. ASME J. Pressure Vessel Technol., Vol. 104, pp. 168-174.
18. Broc, D., Queval, J., and Chaudat, T. 2000. "Fluid Structure Interaction for Nuclear Spent Fuel Racks," ASME Publication, PVP-Vol. 414-2, pp. 171-178.
19. Newman, D., and Karniadakis, G. E. 1996. "Simulations of Flow Over a Flexible Cable: A Comparison of Forced and Flow-Induced Vibration," Journal of Fluids and Structures, Vol. 10, pp. 439-453.
20. Chen, S. S. 1987. "A General Theory for Dynamic Instability of Tube Arrays in Crossflow," J. Fluids Struct., Vol. 1, p. 35-53.
21. Blevins, R. D. 1974. "Fluid Elastic Whirling of a Tube Row," J. Pressure Vessel Technol., Vol. 96, pp. 263-267.
22. Connors, Jr., H. J. 1970. "Fluidelastic Vibration of Tube Arrays Excited by Cross Flow," in Flow-Induced Vibration of Heat Exchangers, ed. D. D. Reiff, ASME, New York, pp. 42-56.
23. Price, S. J., and Paidoussis, M. P. 1983. "Fluidelastic Instability of an Infinite Double Row of Circular Cylinders Subjected to a Uniform Crossflow," ASME J. Vibration, Acoustics, Stress, Reliability Des., Vol. 105, pp. 59-66.

24. Paidoussis, M. P., Price, S. J., and Mavriplis, D. 1984. "A Semi-Potential Flow Theory for the Dynamics of Cylinder Arrays in Cross Flow," Proceedings ASME Symposium on Flow-Induced Vibrations, Vol. 2, ASME, New York, pp. 67-81.
25. Chen, S. S., Zhu, S., and Cai, Y. 1995. "An Unsteady Flow Theory for Vortex-Induced Vibration," J. Sound Vib., Vol. 184(1), pp. 73-92.
26. Granger, S. 1990. "A Global Model for Flow-Induced Vibration of Tube Bundles in Cross-Flow," ASME Publication, PVP-Vol. 189, New York, pp. 139-151.
27. Tanaka, H., and Takahara, S. 1981. "Fluid Elastic Vibration of Tube Array in Cross Flow," J. Sound Vibration, Vol. 77, pp. 19-37.
28. Chen, S. S. 1975. "Vibration of Nuclear Fuel Bundles," Nucl. Eng. Des. 35, 399-422.
29. Chen, S. S., Cai, Y., and Srikantiah, G. S. 1998. "Fluid-Damping-Controlled Instability of Tubes in Crossflow," Journal of Sound and Vibration, Vol. 217(5), pp. 883-907.
30. Weber, D. P., Chen, S. S., Wang, C. Y., Wang, Wei, T. Y. C, and Jansson, S. 2000. "Coupled CFD/CSM Vibration Design Methodology for Generation IV Long-Life Fuel and Component Design," Presented at the Fourth International Conference on Supercomputing in Nuclear Applications, September 4-7, 2000, Tokyo, Japan.
31. Zhu, S., Chen, S. S., and Cai, Y. 1997. "Vibration and Stability of Two Tubes in Crossflow," Journal of Pressure Vessel Technology, Vol. 119, pp. 142-149.
32. Roberts, B. W. 1966. "Low Frequency, Aeroelastic Vibrations in a Cascade of Circular Cylinders," Mechanical Engineering Science, Monograph No. 4.
33. Chen, S. S., Zhu, S., and Cai, Y. 1995. "Experiment of Chaotic Vibration of Loosely Supported Tube Rows in Cross-Flow," J. Pressure Vessel Technol. 117, 204-212.